



A new species of *Diacheopsis* (Myxomycetes) and a new habitat for myxomycetes

Henrik F. Gøtzsche, Bernard Woerly, Flavius Popa, Oleg N. Shchepin, Ilya S. Prikhodko, Ángela López-Villalba, Jan Woyzichovski, Lothar Krieglsteiner, Yuri K. Novozhilov, Anja Klahr & Martin Schnittler

To cite this article: Henrik F. Gøtzsche, Bernard Woerly, Flavius Popa, Oleg N. Shchepin, Ilya S. Prikhodko, Ángela López-Villalba, Jan Woyzichovski, Lothar Krieglsteiner, Yuri K. Novozhilov, Anja Klahr & Martin Schnittler (05 Nov 2024): A new species of *Diacheopsis* (Myxomycetes) and a new habitat for myxomycetes, *Mycologia*, DOI: [10.1080/00275514.2024.2413343](https://doi.org/10.1080/00275514.2024.2413343)

To link to this article: <https://doi.org/10.1080/00275514.2024.2413343>



© 2024 The Author(s). Published with license by Taylor & Francis Group, LLC.



[View supplementary material](#)



Published online: 05 Nov 2024.



[Submit your article to this journal](#)



[View related articles](#)



[View Crossmark data](#)

A new species of *Diacheopsis* (Myxomycetes) and a new habitat for myxomycetes

Henrik F. Gøtzsche^a, Bernard Woerly^b, Flavius Popa^c, Oleg N. Shchepin^{d,e}, Ilya S. Prikhodko^{d,e}, Ángela López-Villalba^d, Jan Woyzichovski^d, Lothar Kriegelsteiner^f, Yuri K. Novozhilov^{d,e}, Anja Klahr^d, and Martin Schnittler^d

^aDrejøgade 19, 3. tv., Copenhagen Ø DK-2100, Denmark; ^bRue des Comtes de Stralenheim 14, Oberbronn F-67110, France; ^cBlack Forest National Park, Seebach D-77889, Germany; ^dInstitute of Botany and Landscape Ecology, Ernst-Moritz-Arndt University Greifswald, Soldmannstr. 15, Greifswald D-17489, Germany; ^eLaboratory of Mycology, V.L. Komarov Botanical Institute of the Russian Academy of Sciences, Prof. Popov St. 2, St. Petersburg 197376, Russia; ^fBrunnenweg 32, Spraitbach D-73565, Germany

ABSTRACT

We describe a new species, *Diacheopsis resinae* (Myxomycetes), collected from a microhabitat new for myxomycetes: stem wounds of coniferous trees (Norway spruce) where the resin is overgrown with a community of resinicolous fungi. The 80 known collections come from the Vosges (France), the Black Forest (Germany), Swabian Alp (Germany), and several localities in Denmark and Norway. Observations, but as well as metabarcoding of substrate samples with fungal (ITS [internal transcribed spacer]), bacterial (16S rDNA), and myxomycete (18S nuc rDNA) primers from eight trunks, revealed the new myxomycete to co-occur with resin-degrading ascomycetes (*Infundichalara microchona*, *Lophium arboricola*, *Zythia resinae*). The gram-negative bacterial genera *Endobacter* and *Sphingomonas* were found to be abundant in the substrate and may be a food source for the myxomycete. Fruit bodies were found mostly during the more humid winter season, with a peak in January/February. Partial sequences of two independent molecular markers (18S nuc rDNA, *EF1a* [elongation factor 1- α] gene) were obtained for 41 accessions, which form a monophyletic cluster in a two-gene phylogeny of Stemonitidales but do not group with other species of *Diacheopsis*, thus rendering this genus paraphyletic. The new species, although exclusively developing sessile sporocarps and morphologically undoubtedly falling into the genus *Diacheopsis*, is most closely related to species of *Lamproderma*, especially *L. album*, *L. zonatum*, and *L. zonatopulchellum*. Within *D. resinae*, three groups can be differentiated, which show nearly complete reproductive isolation, as judged from a recombination analysis of the two unlinked markers and the allelic combinations of the *EF1a* gene.

ARTICLE HISTORY

Received 16 December 2023
Accepted 3 October 2024

KEYWORDS

18S nuc rDNA; Amoebozoa; distribution; *EF1a*; *Lamproderma*; Myxogastria; resinicolous; SEM; taxonomy; 1 new taxon


INTRODUCTION

The genus *Diacheopsis* was erected by Meylan (1930), who described *D. metallica*, a species belonging to the ecological guild of nivicolous myxomycetes discovered by him (Kowalski 1975; Meylan 1908). Fructifications occur at the edge of melting snowbanks, although not exclusively in alpine areas (Ronikier and Ronikier 2009). Nivicolous myxomycetes are members of under-snow microbial communities that need a long, continuous insulating snow cover to form fructifications in the spring with the snow melt (Schnittler et al. 2015). The group comprises around 100 taxa of mostly dark-spored myxomycetes (FioreDonno et al. 2012), such as *Diderma* and *Lepidoderma* (now *Polyschismium*) in the family

Didymiaceae (Prikhodko, Shchepin, Bortnikova et al. 2023; Ronikier et al. 2022) and *Lamproderma* and *Diacheopsis* within the Lamprodermataceae sensu Leontyev et al. (2019).

Diacheopsis Meyl. shares many morphological similarities with *Lamproderma* Rostaf.; the most prominent distinguishing character is the absence of stalk and columella, causing sessile fructifications. Both genera are traditionally included in the order Stemonitales (= Stemonitales) (Kowalski 1968, 1970) and belong to the dark-spored clade of myxomycetes (FioreDonno et al. 2012). In the proposal of Leontyev et al. (2019) for a classification of the myxomycetes, *Lamproderma* is placed in the family Lamprodermataceae within the order Physarales, together with the genera *Diacheopsis*, *Colloderma*, and *Elaeomyxa*, whose relationship to *Lamproderma* is not resolved.

CONTACT Martin Schnittler  martin.schnittler@uni-greifswald.de

 Supplemental data for this article can be accessed online at <https://doi.org/10.1080/00275514.2024.2413343>.

© 2024 The Author(s). Published with license by Taylor & Francis Group, LLC.

This is an Open Access article distributed under the terms of the Creative Commons Attribution-NonCommercial-NoDerivatives License (<http://creativecommons.org/licenses/by-nc-nd/4.0/>), which permits non-commercial re-use, distribution, and reproduction in any medium, provided the original work is properly cited, and is not altered, transformed, or built upon in any way. The terms on which this article has been published allow the posting of the Accepted Manuscript in a repository by the author(s) or with their consent.

The genus *Diacheopsis* currently comprises 19 species recognized by Lado (2005–2023). Of these, six species are nivicolous, four are corticolous, and the remaining species are litter inhabiting, xylobionts, or those of which habitat preferences cannot be inferred from the few known observations.

This study describes a taxon in the genus *Diacheopsis* from numerous localities in Denmark, France, Germany, and Norway with an ecological niche new for myxomycetes: stem wounds of Norway spruce (*Picea abies*) where the resin overgrown with a community of resinicolous fungi. Using two independent markers (18S nuc eDNA as a barcoding marker established for myxomycetes and the *EF1α* [elongation factor 1- α] gene as an independent second marker), we aim (i) to ascertain the systematic position of the new species by a combination of both markers, (ii) to exclude morphologically similar species via the 18S nuc rDNA barcodes, the gene sequenced most often for myxomycetes, and (iii) to reveal the internal genetic structure of the new taxon by recombining sequence variants (multilocus “fields for recombination” [Doyle 1995]; see example in Flot et al. 2010). To investigate the composition of bacterial and fungal communities in the new microhabitat and to confirm the presence of vegetative stages of the myxomycete, we employ metabarcoding for fungi and bacteria via the established barcoding markers ITS (internal transcribed spacer) and 16S rDNA, respectively.

MATERIALS AND METHODS

Collection sites and field sampling.—The new species was mostly found in three countries and two regions of Europe: the Vosges Mountains and the Black Forest (France/Germany, separated by the ca. 70 km wide valley of the Rhine) and in lowland forests in Denmark. In addition, three records are known from Norway (SUPPLEMENTARY FILE 1).

The Vosges are a mid-elevation (up to ca. 1400 m above sea level [a.s.l.]) mountain massif in northeastern France; bedrocks include sandstone and granite of Hercynian origin. The climate is humid and temperate, with rather high precipitation (990 mm, station Mouterhouse, 270 m; data 1981–2010, Météo-France 2023), but figures for the summits exceed 2000 mm. Forests are mainly composed of Scots pine, oak, and beech in lower regions, whereas spruce and fir dominate in higher regions. Significant proportions of planted spruce, especially in the valleys, offer a refuge for deer, which frequently cause stem wounds in spruce trees through which the resin drains.

Very similar in altitude, bedrock composition, climate, and vegetation is the Black Forest. Precipitations are also high for the German counterparts (annual mean 2000–2200 mm); the annual temperature is only 5–6 °C for the plateau around 1000 m a.s.l.

The locations in Denmark, central and southern Jutland, are situated on diluvial plains, created during the melting period after the last glaciation. The soils are sandy and generally poor, often with sand dunes scattered inland and covered with trees. The eastern localities, on the Djursland peninsula and the island of Zealand, are generally on more fertile soils, mostly moraines. All collecting sites were in spruce plantations, below ca. 100 m a.s.l.

Morphological analyses.—The Danish collections upon which the morphological description is based were studied with a Zeiss Jena stereomicroscope (Oberkochen, Germany) and a Leica DM1000 LED compound microscope (Wetzlar, Germany). Microscopic measurements were made at 1000 \times in water with detergent added. A total of 25–30 spores from each collection were measured to the nearest 0.5 μ m; measurements were exclusive of ornamentation. Micrographs of spores were made with a 100 \times oil immersion objective, numerical aperture (NA) 1.25; white balance was adjusted on slide with no objects. Macro images were made with a Canon EOS 500 SLR camera (Tokyo, Japan) with a Zeiss Distagon 28/2.8 objective mounted in reverse position and 0.5–3.5 cm extension.

Macrographs of the German specimens were taken with a Keyence VHX-7000 digital dissecting microscope (Keyence, Osaka, Japan). Scanning electron microscopy (SEM) of the spores was carried out with a Zeiss DSM950 microscope at the University of Alcalá (Spain) after applying the critical-point-drying technique, following the methodology described in López-Villalba et al. (2022). SEM micrographs of the capillitium and peridium were taken with a Zeiss EVO LS10 microscope without prior critical point drying.

A quantitative measurement of spores was carried out for 22 specimens as described in Woyzichovski et al. (2021, 2022), including a minimum of 200 spores per sporocarp.

DNA extraction, amplification, and sequencing.—Extraction of genomic DNA was done with ca. 400 spores sampled from a single sporocarp (18S nuc rDNA) or from 2–5 whole sporocarps (*EF1α* gene) according to the protocols described in Schnittler et al. (2020) and Prikhodko, Shchepin, Bortnikova et al. (2023a), respectively. For partial sequences of the 18S nuc rDNA, the first part of the small

subunit that is free of introns (cf. fig. 4 in Fiore-Donno et al. 2012) was targeted by the primer pair S2 (Fiore-Donno et al. 2008) and SU19R (Fiore-Donno et al. 2011) or SSU_rev (Prikhodko, Shchepin, Bortnikova et al. 2023). Partial sequences of the gene for the protein elongation factor *EF1 α* (amino acids 120–370; see SUPPLEMENTARY FILE 5) were amplified with the primer pair PB1F/PB1R (Novozhilov et al. 2013) in case of Lamprodermataceae sensu Leontyev et al. (2019). For Amaurochaetaceae, a combination of primers for a seminested PCR (EF03 [or EF04] and KEF_R3; Ronikier et al. 2020; Wrigley de Basanta et al. 2017) was used; for amplification conditions, see Prikhodko, Shchepin, Bortnikova et al. (2023).

Protocols for polymerase chain reactions (PCRs) and purification are as in (Prikhodko, Shchepin, Bortnikova et al. (2023) and Prikhodko, Shchepin, Gmshinskiy et al. (2023) and Schnittler et al. (2020), but for the latter approach we used the AccuStart premanufactured master mix (QuantaBio, Beverly, Massachusetts) with a final volume of 20 μ L. PCR products were purified with alkaline phosphatase (Thermo Fisher) or a magnetic bead-based kit (NimaGen D-Pure DyeTerminator Cleanup Kit; Nijmegen, the Netherlands) and analyzed on ABI 3130/3500 automated DNA sequencers (Applied Biosystems, Foster City, California).

Sequence alignment and phylogenetic analyses.—

Taxon sampling for the two-gene phylogeny of Physarales sensu Leontyev et al. (2019) focused on the genera *Lamproderma* and *Diacheopsis* (see SUPPLEMENTARY FILE 1). The resulting two-gene phylogeny from 203 sequences was rooted with *Barbeyella minutissima* and *Echinostelium bisporum* from the order Echinosteliales, occupying the most basal position within the group of dark-spored myxomycetes (Columellomycetidae; Leontyev et al. 2019).

18S nuc rDNA and *EF1 α* partial sequences were compiled in Unipro UGENE (Okonechnikov et al. 2012) and aligned using MAFFT online service (Katoh et al. 2019; Katoh and Standley 2013) with E-INS-i or G-INS-i options, respectively, and default gap penalties. After primer trimming and manual editing, alignments were merged with SequenceMatrix 1.9 (Vaidya et al. 2011). The 18S nuc rDNA sequences were analyzed as a single partition, whereas two separate partitions were defined for the *EF1 α* sequences: the first and second positions of each codon, which tend to be more conservative, were analyzed separately from the third position, where most of the mutations are synonymous. The exon parts of the *EF1 α* sequences were determined

according to the sequence from *Echinostelium bisporum* (GenBank MH814572) obtained from transcriptome data (Fiore-Donno et al. 2018).

The final alignment consisted of 203 sequences with 2687 sites, 1367 distinct patterns, 308 singleton sites, and 1521 noninformative (constant) sites (SUPPLEMENTARY FILE 2). Maximum likelihood (ML) analyses were performed using IQ-TREE 1.6.12 (last stable release; Nguyen et al. 2015) launched on the local machine. The TIM2e+I+G4 model was selected for the 18S nuc rDNA partition according to the ModelFinder tool implemented in the program (Kalyaanamoorthy et al. 2017). HKY+F+R6 and GTR+F+I+G4 models were selected for the first two and third positions of each codon in *EF1 α* partitions, respectively. Ultrafast bootstrap analysis with 1000 replicates (Hoang et al. 2018) was performed to obtain confidence values for the branches. Bayesian analysis was performed with the same data set using MrBayes 3.2.7a (Huelsenbeck and Ronquist 2001) run on CIPRES Science Gateway (Miller et al. 2010); the GTR+G+I model was applied. The phylogenetic analysis was done in four independent runs, each consisting of four separate chains sampled over 20 million generations (sampling every 1000). The convergence of Metropolis-coupled Markov Chain Monte Carlo (MCMCMC) was estimated using Tracer 1.7.2 (Rambaut et al. 2018); based on the estimates by Tracer, the first 5 million generations were discarded as burn-in. Posterior probabilities (PPs) of splits were exported to the best-scoring ML tree using -sup option in IQ-TREE. The phylogenetic tree with combined supports was visualized for FIG. 1 using FigTree 1.4.4 and edited using Corel Draw 24.0 (Alludo, Ottawa, ON).

To compare the identity of the DNA barcodes of the new species with that of other *Diacheopsis* and *Lamproderma* spp., a BLAST search was conducted. A total of 270 partial 18S nuc rDNA sequences were sampled and aligned using MAFFT online service with E-INS-i strategy and default gap penalties (SUPPLEMENTARY FILE 3). The model TIM2e+I+G4 was selected using the ModelFinder tool according to Bayesian information criterion (BIC). A maximum likelihood tree search was performed with 1000 ultrafast bootstrap replicates in IQ-TREE 1.6.12 (SUPPLEMENTARY FIG. 4).

A separate phylogeny was reconstructed for the *EF1 α* sequences using the same alignment and substitution model as for the two-gene phylogeny. A maximum likelihood tree search was performed with 1000 ultrafast bootstrap replicates in IQ-TREE 1.6.12 (SUPPLEMENTARY FIG. 5).

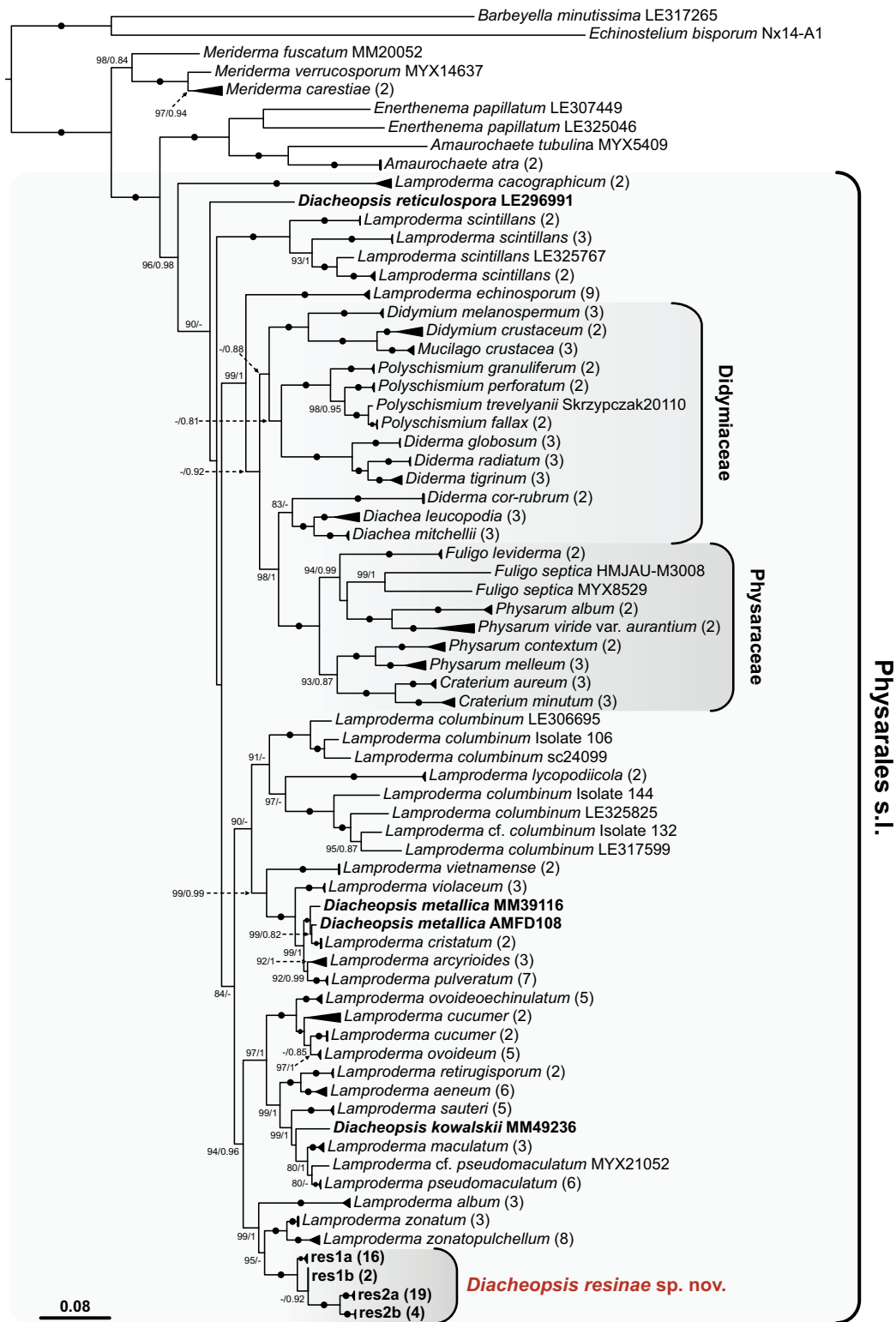


Figure 1. Two-gene phylogenetic tree of Physarales sensu Leontyev et al. (2019) obtained with a maximum likelihood analysis of partial 18S nuc rDNA and *EF1a* and rooted with species of the Echinosteliaceae (*Barbeyella*, *Echinostelium*). Names for species of *Diacheopsis* are written in bold. A triangle depicts contracted clades (with its length equivalent to the average length of the branches in the contracted clade); numbers in parentheses indicate the number of accessions in the respective clade. All sequences from specimens belonging to the same taxon that differ in less than 0.04 nucleotide substitutions per site were contracted. The internal structure of the new species is shown with higher resolution (groups *res2a* and *res2b* differ in less than 0.04 substitutions). Branch supports are shown only for ultrafast bootstrap replicates/Bayesian posterior probabilities $\geq 80/0.9$; black dots indicate maximum supports in both analyses; the scale bar represents the mean number of nucleotide substitutions per site.

Recombination analysis.—A total of 44 isolates of the new species were sequenced for *EF1 α* , showing up to 40 single-nucleotide polymorphisms (SNPs) within the analyzed partial sequence 735 bp long (corresponding to 245 amino acids); see SUPPLEMENTARY FILE 5. To explore possible signs of reproductive isolation, the alleles of the nuclear marker *EF1 α* were reconstructed using a Python 3 script (Shchepin 2023) with an iterative procedure based on the maximum parsimony principle. First, it checked whether any of the heterozygous sequences could be explained by combining two known alleles. Then it tried to find heterozygous sequences that could result from a combination of one of the known alleles and an unknown allele that could be recovered from their overlap. This process was repeated until no new alleles were derived. If there were any heterozygous sequences that could not be explained by known or recovered alleles and they contained only one heterozygous position, such sequences were unambiguously phased into two alleles. Finally, if the remaining sequences contained more than one heterozygous position, alleles for such sequences were resolved arbitrarily. SUPPLEMENTARY FILES 6 and 7 show the resulting alleles and a table of results.

The retrieved alleles were compared with the 18S nuc rDNA sequences of the respective specimens to analyze combinations of ribotypes/alleles (SUPPLEMENTARY FILES 4/6) for the two markers, and the result was visualized with a Python 3 script (FIG. 2C; Shchepin 2021). After that, a “haploweb” was constructed using the same approach as in Flot et al. (2010). In brief, the alleles found for the *EF1 α* sequences were used to produce a network showing their genetic distances, and the network was overlaid with the observed combinations of alleles (FIG. 2D).

Metabarcoding analysis of associated communities.

—Species identification in organic material of stem wounds from 8 spruce trees was attempted by DNA metabarcoding, following a protocol published in Hausmann et al. (2020) for bacteria and fungi and a modified protocol from Borg Dahl et al. (2019) for dark-spored myxomycetes. Material was sampled in the Black Forest National Park at the sites Herrenwies 1 (*Diacheopsis* voucher KR-M-0092822), Vogelskopf (metabarcoding voucher KR-M-0093591, *Diacheopsis* voucher KR-M-0092862), Hundseck (*Diacheopsis* voucher KR-M-0092824), Ruhestein 1 (*Diacheopsis* voucher KR-M-0092865), Darmstädter Hütte 1 (*Diacheopsis* voucher sc32566), Darmstädter Hütte 3 (metabarcoding voucher KR-M-0093640, *Diacheopsis* only observed),

Hoher Ochsenkopf 1 (metabarcoding voucher KR-M-0093590, *Diacheopsis* voucher KR-M-0092869), and Hoher Ochsenkopf 2 (*Diacheopsis* voucher KR-M-0092870).

The layer with the microbial community inhabiting the stem wounds (see FIG. 3B) was scraped directly from the spruce resin to reduce the amount of pure resin in the sample. The material was dried at 60 C for 8 h and subsequently homogenized in a FastPrep-96 homogenizer (MP Biomedicals, Thermo Fisher Scientific, Waltham, Massachusetts), using sterile steel beads in order to generate a homogeneous mixture of organic material to be submitted for subsequent metabarcoding (conducted by AIM—Advanced Identification Methods, Leipzig, Germany). Prior to DNA extraction, 1 mg of each homogenizate was weighed into sample vials and processed using adapted volumes of lysis buffer with the DNeasy 96 Blood & Tissue Kit (Qiagen, Venlo, Netherlands) following the manufacturer’s instructions. Primers and amplification of the target regions (ITS2 for fungi [Toju et al. 2012], 16S rDNA for bacteria [Thijs et al. 2017], 18S nuc rDNA for myxomycetes [Borg Dahl et al. 2019]) using a two-step PCR (Morinière et al. 2016), preparation of the MiSeq libraries, sequencing with Illumina MiSeq, and bioinformatics processing of raw reads using the VSEARCH suite 2.9.1 (Rognes et al. 2016) and Cutadapt 1.18 (Martin 2011) are described in detail in SUPPLEMENTARY FILE 10.

For bacteria and fungi, operational taxonomic units (OTUs) were clustered at a 97% similarity threshold. To select the most important OTUs for data evaluation, weighted abundance (total number of reads \times frequency in the eight samples, a number between 1 and 8) was calculated for each OTU. The OTUs with the highest weighted abundance were selected, until 50% of the sum of all weighted abundances was reached (see SUPPLEMENTARY FILE 8).

For myxomycetes, amplicon sequence variants (ASVs) were clustered at 100% similarity threshold in the process of sequence denoising, preserving every unique 18S nuc rDNA barcode sequence that survived filtering steps. Since the same approach to the selection of the most important ASVs using the weighted abundances that was applied to bacterial and fungal OTUs would result in only three selected ASVs of myxomycetes, 50 ASVs with the highest number of reads were selected for the analyses instead (SUPPLEMENTARY FILE 9). ASV sequences were aligned to the 18S rDNA data set (SUPPLEMENTARY FILE 11), and a maximum likelihood phylogeny (SUPPLEMENTARY FIG. 5) was reconstructed using the same methodology as for SUPPLEMENTARY FIG. 4.

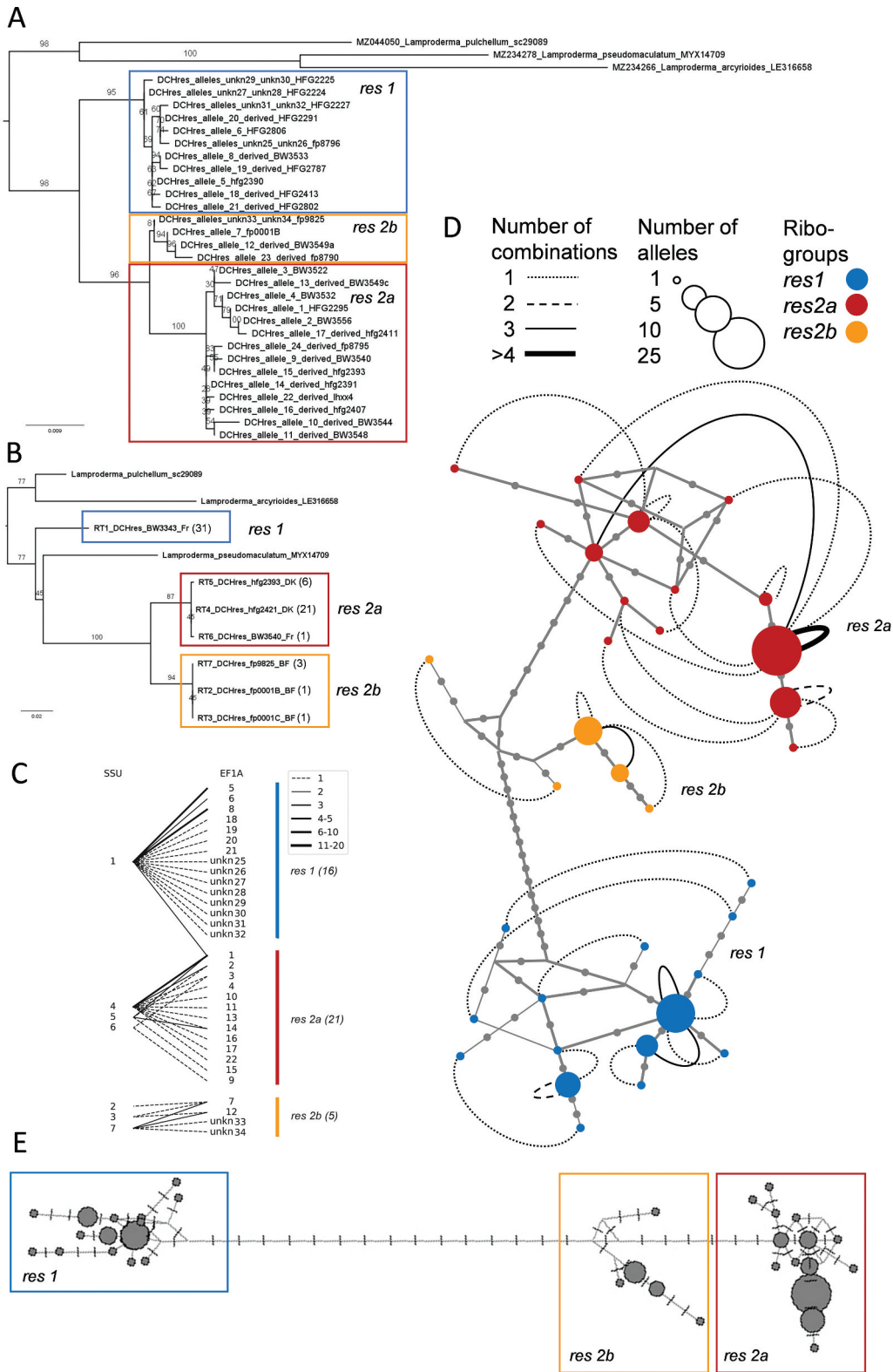


Figure 2. Intraspecific diversity within *Diacheopsis resiniae*. Consistently, three groups are visible, which were color-coded with blue for *res1*, red for *res2a*, and gold for *res2b*. (A, B) Maximum likelihood trees (A) for all 34 alleles found for the *EF1a* marker from 44 specimens (10 arbitrarily phased alleles with “unkn” in the label are presented here as five heterozygous unphased sequences) and (B) for seven ribotypes found within 64 specimens. (C) Recombination analysis of the two marker genes. Line type indicates the number of combinations (specimens homozygous for *EF1a* were counted twice). (D) Network of reconstructed *EF1a* alleles with the hypothetical mutational steps between them (one SNP equals one mutation) marked by ticks on the straight lines. Curved lines connect alleles occurring in one (dotted), two (hatched), three (solid), or more (bold) specimens. Alleles 1–7 were found in homozygous state, alleles 8–24 were derived from heterozygous specimens assuming one allele corresponds to alleles 1–7, and alleles 25–34 represent hypothetical alleles that could not be unambiguously derived since two of them occur together. (E) The same network drawn to scale (mutational steps) to visualize genetic distances between alleles.

TAXONOMY

Diacheopsis resinae Woerly & Gøtzsche, sp. nov.
FIGS. 3–4

MycoBank MB849308

Typification: DENMARK. JYLLAND: Søndre Feldborg Plantage, at Visborgvej, ca. 40–50-year-old plantation of *Picea abies*, 56.31606°N, 8.96119°E, on a large wound made by *Cervus elaphus* (red deer) on a spruce stem, ca. 1–2 m above the ground, 1 Dec 2013, leg. H.F. Gøtzsche & N.V. Mogensen (**holotype** hfg2408, phylogroup *res2a*; GenBank: 18S nuc rDNA = OR783613, *EF1α* = OR778653), deposited at M; isotypes (duplicates of hfg2408) are in the private herbaria of H. F. Gøtzsche and B. Woerly.

Other specimens examined: See SUPPLEMENTARY FILE 1.

Etymology: *resinae* refers to the resin in stem wounds degraded by fungi, where the species was found and which is a rather unusual substrate for Myxomycetes (FIG. 3A, B).

Description: Fruit bodies sessile, solitary to grouped, in groups of 2–10(–30), developed as cushion-shaped small sporocarps with a constricted base, 0.5–1 mm to often irregularly shaped plasmodiocarps up to 3 mm long and 2 mm wide. Peridium thin, membranous, lead gray, and often with metallic iridescence by reflected light (FIG. 3D, E), almost hyaline to smoky by transmitted light (FIG. 3G) with a darker base, on the outside occasionally with microscopic rod-shaped crystals that do not dissolve in HCl, sprinkled randomly on the surface, inner side nearly smooth (FIG. 4F), dehiscing irregularly. Hypothallus very inconspicuous, sometimes visible as a thin, shiny layer between fruit bodies. Capillitium blackish to brown in transmitted light, hyaline at the free endings, creating a three-dimensional net at the base of the sporocarp that radiates to the peridium, threads 1–3 µm diam, solid, straight to moderately undulate, smooth to slightly roughened, bifurcated and sometimes with perpendicular ramifications, with dark spindle-shaped expansions up to 80 µm long and 8 µm wide (FIGS. 3H–G, 4A, E). Spores globose, in the holotype 14–15.13–17 µm diam (min–mean–max, $n = 30$, excluding ornamentation). Quantitative measurements show considerable variation between specimens (14.8–15.8 to 17.1–17.8 µm for the 25/75% quantiles; SUPPLEMENTARY FIG. 2). Spore mass very dark brown to almost black by reflected light, spores medium grayish brown by transmitted light with one half distinctly paler, with dark, regularly distributed blunt spines up to 0.5 µm high, spines are less prominent at the paler side (FIGS. 3I, 4B–D). Plasmodium probably whitish, as the developing fruit bodies (FIG. 3C).

Diagnosis: A combination of characters tells the species apart from other *Diacheopsis* spp.: parallel capillitial threads arising from the entire base of the sporocarp and rather large spores with blunt spines.

Comments: According to the generic description of *Diacheopsis* (Martin and Alexopoulos 1969; Meylan 1930), the new species clearly falls into that genus based on morphological characters, since the sporocarps are sessile, the peridium is persistent and iridescent, the columella is absent, the capillitium is branched, and the capillitium and spores are dark. It joins the group of rare, large-spored, spinulose, non-nivicolous species of *Diacheopsis*. Based on Lado (2005–2023) and Poulain et al. (2011), this group comprises currently the following species: *D. insessa* (G. Lister) Ing, *D. mitchellii* Nann.-Bremek. & Y. Yamam., and *D. gigantospora* Shuang L. Chen, M. Q. Guo & S.Z. Yan. *Diacheopsis insessa* is in spore diameter very similar to *D. resinae* but possesses an outer three-dimensional capillitium net, in contrast to the mostly parallel branches of *D. resinae*, which only forms a net at the base of the sporotheca. The 18S nuc rDNA sequence of *D. insessa* is very different from all barcodes of *D. resinae*. Also macroscopically similar is *D. mitchellii*, but the frayed spines of the spores clearly distinguish it from *D. resinae*, which has spores with short, sometimes blunt, spinules (FIG. 4B–D). Although the spore size of *D. resinae* shows significant variation (SUPPLEMENTARY FIG. 2), only exceptionally single spores reach the interval of 20–21 µm reported for *D. mitchellii* or 20.6–26.2 µm for *D. gigantospora*. The latter species was cultured on bark of *Cryptomeria* at room temperature and seems to be corticolous. In addition, *D. resinae* differs from all known species of myxomycetes by its unique microhabitat.

Molecular data point toward two, perhaps three, phylogroups that seem to be reproductively isolated and can be seen as putative biospecies. These three groups do not show a geographic differentiation (SUPPLEMENTARY FIG. 1). We could not discover prominent differences between them in habit or microscopic characters. For groups *res1* and *res2a*, we had enough material for a quantitative measurement of spores (SUPPLEMENTARY FIG. 2) but could not find clear differences in spore size, as it is the case for spore ornamentation (FIG. 4B–D).

Distribution: The new species is currently known from northern (Norway: Vestfold og Telemark, Innlandet, Viken; Denmark: Jutland, Zealand) and central (France: Vosges, Alsace; Germany: Black Forest, Swabian Alps, both in Baden-Württemberg) Europe

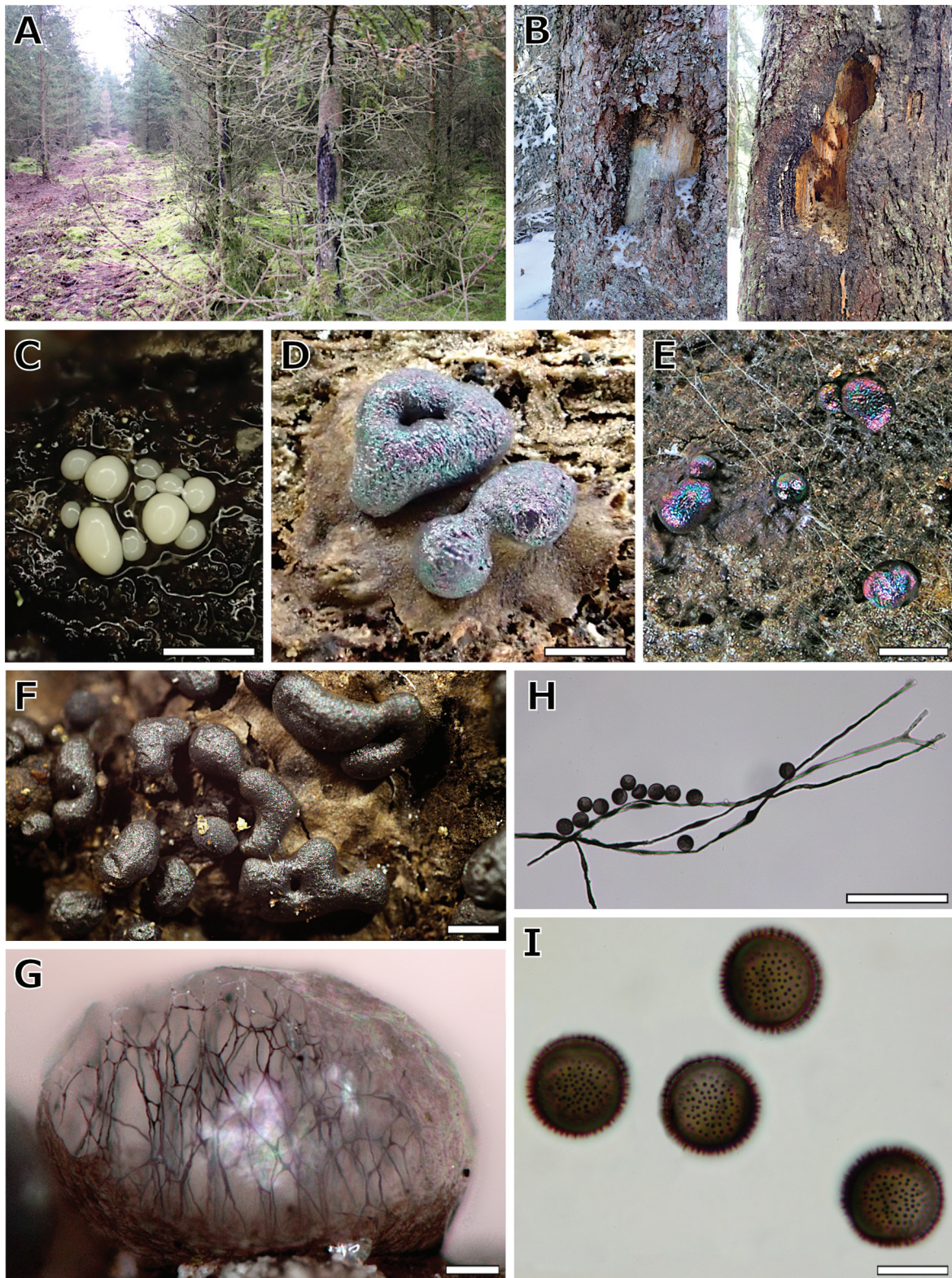


Figure 3. Habitat and morphology of *Diacheopsis resinae*, sp. nov. (A) Danish spruce plantation with a wounded tree in the foreground (habitat of the first records made, hfg2217 and hfg2218). (B) Close-up of the habitat (Black Forest): stem wounds in spruce trunks (*Picea abies*) covered with resin. (C) Fresh, immature sporocarps covered by a slime sheath (same tree as KR-M-0092863). (D) Young sporocarps; desiccation reveals a membranous, iridescent peridium (sc32566). (E) Iridescent peridium in well-matured sporocarps (P1013032). (F) Change of color on mature and somewhat sclerotized plasmodiocarps (HFG2408). (G) Detail of a sporocarp with blown-up spores, showing the hyaline peridium and the capillitium threads rising from the bottom to the top of the sporocarp (9926 CF). (H) Spores and capillitium in transmitted light (HFG2408). (I) Spores in transmitted light (HFG2408), stacked from two photographs showing the spore surface and the spore margin, respectively. Bars: C, E, F = 1 mm; D = 0.5 mm; G, H = 100 μ m; I = 10 μ m. For more images, see <http://www.myx.dk/spp/disres.html>.

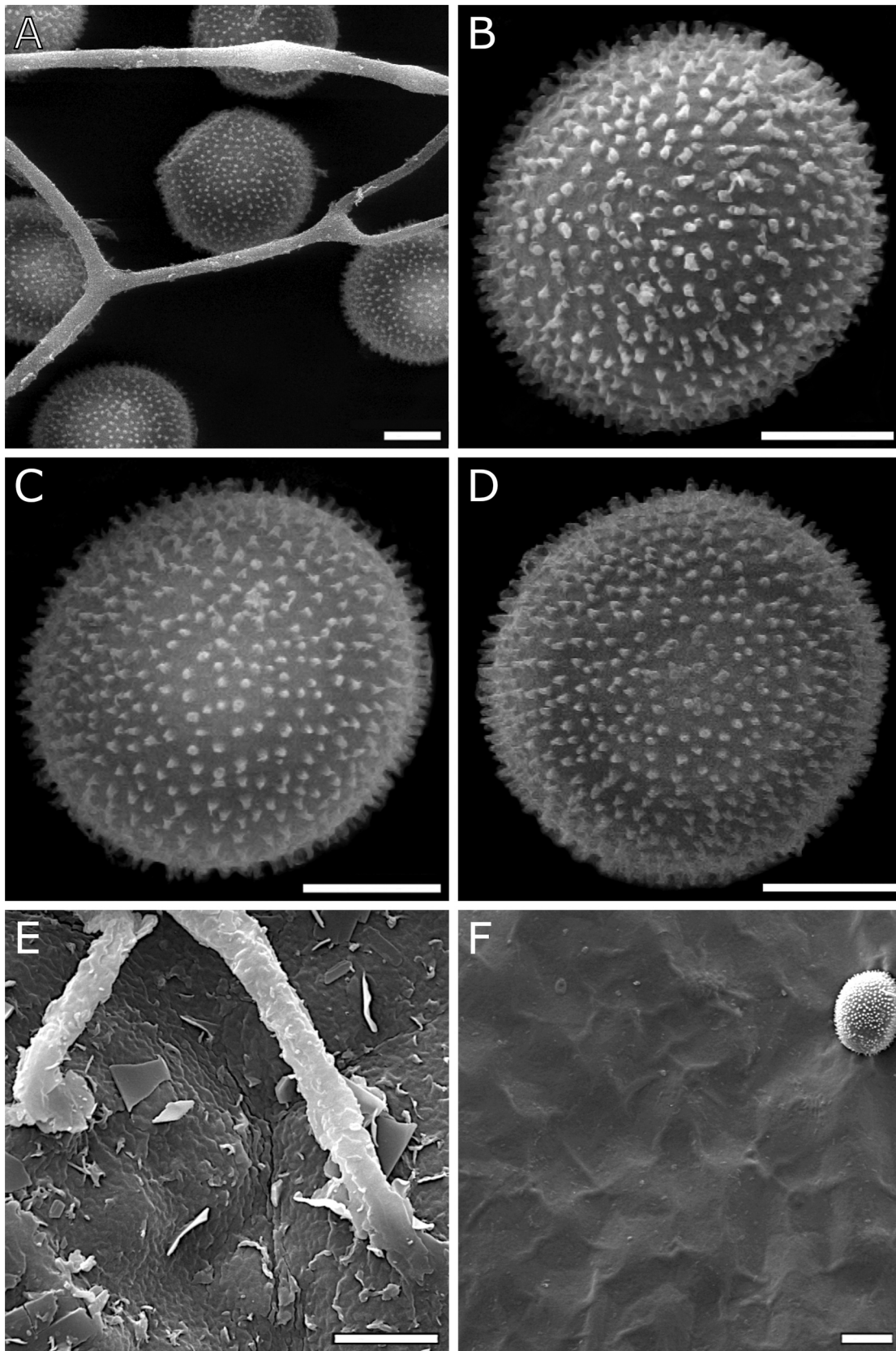


Figure 4. SEM micrographs of *Diacheopsis resinae*, sp. nov. (A) Spores and capillitium (fp8799). (B–D) Spores of specimens BW3368b (*res1*), BW8789 (*res2a*), and fp0001B (*res2b*), respectively. (E) Connections between the capillitium and the inner side of the peridium (collection 9926 CF). (F) Smooth, outer side of the peridium (collection BW3368b). Bars: A–E = 5 µm; F = 20 µm.

(SUPPLEMENTARY FILE 1). Searches in the German Alps (Bavaria), the French Pyrenees, and the Romanian mountains (Făgăraș, Munții Piatra Craiului, Apuseni) were not successful so far.

Ecology: Found exclusively on resin-clad stem wounds of Norway spruce (*Picea abies*), which constitute a new microhabitat for myxomycetes (SUPPLEMENTARY FILE 1).

RESULTS

Systematic position of the new taxon.—To infer the phylogenetic position of the new species, we constructed a two-gene phylogeny (18S nuc rDNA, *EF1α*) of Physarales sensu Leontyev et al. (2019), considering especially Lamprodermataceae (*Diacheopsis* 3 taxa, *Lamproderma* 21 taxa) and 41 accessions of the new species (FIG. 1; SUPPLEMENTARY FILE 2).

The overall topology of the two-gene phylogeny is congruent with other studies (e.g., Fiore-Donno et al. 2012), with *Meriderma* spp. as the basal clade of dark-spored myxomycetes (ultrafast bootstrap replicates/Bayesian posterior probabilities 98/0.84), followed by members of the Amaurochaetaceae (here the genera *Enerthenema* and *Amaurochaete* form a branch with maximum support). *Lamproderma cacographicum* appears as a basal taxon of Physarales s.l. (100/1). This fact, as well as the nestedness of Didymiaceae and Physaraceae within *Lamproderma* spp., makes this morphologically well-defined genus a paraphyletic taxon (Fiore-Donno et al. 2012; Novozhilov, Shchepin et al. 2022; Prikhodko, Shchepin, Bortnikova et al. 2023; Prikhodko, Shchepin, Gmoshinskiy et al. 2023).

The genus *Diacheopsis* appears polyphyletic in our phylogeny. All three taxa of this genus for which we could obtain both 18S nuc rDNA and *EF1α* sequences appear at different positions in the tree, two of them with high support. The new species, *Diacheopsis resinae*, forms a monophyletic clade maximum support in a sister position to *L. zonatum* and *L. zonatopulchellum*, a species recently described by Yatsiuk et al. (2023). Three of the four subclades within *D. resinae* (called *res1a*, *res2a*, and *res2b* in FIG. 1) also received maximum support.

The separate gene trees for *EF1α* and 18S nuc rDNA are mostly congruent in the topology of statistically supported clades with each other and with the two-gene phylogeny, but with a few exceptions. *Lamproderma lycopodiicola* is grouped with *L. cacographicum* in the 18S nuc rDNA tree, but with *L. columbinum* in the *EF1α* tree (SUPPLEMENTARY FIGS. 4 and 5). In both trees, the genus *Diacheopsis* appears polyphyletic and all sequenced accessions of *Diacheopsis resinae* group together into

a monophyletic clade sister to *L. zonatum* and *L. zonatopulchellum*.

With the exception of *D. metallica*, most of the 19 described species (Lado 2005–2023) of the genus *Diacheopsis* are rare; a typical example is *D. cinerea* (Vlasenko et al. 2022) described from two specimens from the same locality in Siberia. We were able to obtain 18S nuc rDNA barcodes from eight taxa of *Diacheopsis*. In an 18S nuc rDNA phylogeny with various other taxa of Lamprodermataceae (SUPPLEMENTARY FIG. 4), these species (i) appear to be distinct from *D. resinae* and (ii) occur at different positions within the tree. *D. resinae* shows only 90–93% identity to barcodes of its closest match, *Lamproderma pulchellum*. Among the other species of *Diacheopsis*, the position of *D. metallica* (14 accessions from France) is characterized best. In the 18S nuc rDNA phylogeny, it clusters together with specimens of *Lamproderma arcyrrioides*, *L. pulveratum*, and *L. cristatum* (SUPPLEMENTARY FIG. 4), and the barcodes of *D. metallica* are in several cases identical to the abovementioned species of *Lamproderma*. The same is true for two accessions from France that were determined as *D. pauxilla* (MM16552) and *D. reticulospora* (MM21082) (SUPPLEMENTARY TABLE 1).

Intraspecific variation.—Of the 80 total accessions of the new species, 64 could be barcoded for the 18S nuc rDNA marker (SUPPLEMENTARY FILE 3). Seven ribotypes (RTs) were found, and they formed two clearly defined groups in a phylogeny for this marker (FIG. 2B), with the second group splitting again into two subgroups (SUPPLEMENTARY FILE 4). Ribogroup 1 (*res1*) consists of a single ribotype, RT1, identical in 31 specimens. Ribogroup 2a (*res2a*) is represented by eight specimens and three ribotypes. It deviates from *res1* by 37 SNPs and one indel, all located in helices 11, E-10, and 10 of the 18S nuc rDNA (cf. fig. 4 in Fiore-Donno et al. 2012). Ribogroup 2b (*res2b*) deviates from the latter by 23 SNPs and consists of five specimens that belong to three closely related ribotypes that differ only in one indel and one heterozygous position. The two most common ribogroups (*res1*, *res2a*) are both represented by specimens from all three sampled regions.

Due to the often scanty material, only 44 specimens could be successfully sequenced for the *EF1α* gene (18 for *res1*, 19 for *res2a*, four for *res2b*, and for the remaining three no 18S nuc rDNA sequences could be obtained; SUPPLEMENTARY FILE 5). Most but not all specimens (28, 68%) are heterozygous for this marker. This allowed us to derive the respective allelic variants computationally (SUPPLEMENTARY FILES 6, 7): seven were found in homozygous state,

17 hypothetical variants could be derived from heterozygous sequences, and 10 more variants were recovered from heterozygous sequences arbitrarily, assuming the closest match to a sequence already known. Like for the 18S nuc rDNA, a phylogeny for the alleles (FIG. 2A) reveals also two major groups, with the second clade splitting into two subgroups, *res2a* and *res2b*.

If we investigate the combinations between the variants of these two unlinked markers (FIG. 2C), the combinations of 18S nuc rDNA ribotypes and *EF1α* alleles sort the specimens of *D. resinae* into three recombination groups corresponding to the clades *res1*, *res2a*, and *res2b*, forming three mostly mutually exclusive pools of alleles and indicating a high degree of reproductive isolation between these clades. Only two specimens (BW3343 and BW3360, both ribotype 1 and *EF1α* genotype 1; FIG. 2C) represent between-group recombinations, and these two specimens of ribogroup *res1* constitute the clade indicated as *res1b* with low support in FIG. 1. We thus can label the subgroups in the *EF1α* tree as well with the codes derived from the 18S nuc rDNA sequences, since this division appears also in a phylogenetic network of the *EF1α* alleles (FIG. 2D). Here, heterozygous specimens (represented by curved lines) connect only alleles belonging to the same group. If this network is drawn to the scale of mutational steps connecting allelic variants (FIG. 2E), it becomes visible that genetic distances between groups are almost always larger than the maximum within-group distance.

Ecology, phenology, and association with other species.—All known collections of the new species have been found on wounds on trunks of *Picea abies*, inflicted not only by red deer seeking access to the cambium in winters where other food sources were scarce but also by woodpeckers, forest management, fallen neighboring trees, or lightning. The three Norwegian records come from forests naturally inhabited by spruce, whereas all 27 Danish collections were made in rather dense spruce plantations, often with trees below 20 years in age. In the Vosges and the Black Forest, spruce also occurs naturally but was very often planted. Most observations of the new species were made from October to May, with a peak in February (SUPPLEMENTARY FIG. 3).

Within a couple of years, the resin exudated from stem wounds is colonized by various fungi, turning the resin black. *Diacheopsis resinae* co-occurs with this peculiar fungal community (FIG. 5). The substrate is always completely overgrown with a velvety, brownish to blackish mycelium that seemingly represents

a mixture of anamorphic states of different fungal species, with *Sorocybe resinae* (Fr.) Fr. (e.g., Seifert et al. 2007), *Infundichalara microchona* (W. Gams) Réblová & W. Gams, and *Lophium arboricola* (Buczacki) Madrid & Gené especially abundant. Other associated species are the following: the teleomorphs of *Claussenomyces* spp. (FIG. 5A), with thick, gelatinous, green to dark apothecia 0.2–1 mm diam); *Lachnellula resinaria* (Cooke & W. Phillips) Rehm (FIG. 5B), with short stalked apothecia, outer side whitish, inner side yellow-orange, 0.5–1.5 mm diam, but in dry state only the outer side is visible, looking like a small white-pubescent sphere, after Hansen and Knudsen (2000); *Zythia resinae* (Fr.) P. Karst. (FIG. 5C), with sessile, yellow to pale orange apothecia 0.5–1.5 mm diam, after Hawksworth and Sherwood (1981); *Sarea difformis* (Fr.) Fr. (FIG. 5D), with sessile, black apothecia 0.2–1.3 mm, after Mitchell et al. (2021); and, more rarely, *Lophium mytilinum* (Pers.) Fr. (FIG. 5E), with black ascocarps up to 1 mm diam, conchate, with a striated surface, after Ellis and Ellis (1985) and Boehm et al. (2009).

During a structural complexity enhancement experiment conducted in 2016 in the Black Forest National Park (Asbeck et al. 2023), a total of 60 trees in six plots were girdled. Resin at the wounds of all girdled trees was found in 2023 to be overgrown with the typical black mycelium of resinicolous fungi. In spring of the same year, we first observed mature *D. resinae* at three of the 60 trees, occurring 6–7 years after the trees were girdled (vouchers KR-M-0094491, KR-M-0094492).

Metabarcoding detected a total of 319 fungal OTUs (SUPPLEMENTARY FILE 8; TABLE 1). According to the proportion of weighed abundances (total number of reads × frequency among the samples), the most common fungi are *Sarea difformis* (11.4%), *Infundichalara microchona* (10.7%), *Lophium arboricola* (10.4%), *Sorocybe resinae* (8.9%), *Zythia resinae* (5.6%), and an unknown species from the order *Chaetothyriales* (4.5%). *Lachnellula resinaria* and *Lophium mytilinum* were detected as well but with considerably lower steadiness.

In addition, 430 bacterial OTUs (SUPPLEMENTARY FILE 8; TABLE 1). Most prominent were two species from the genera *Endobacter* (21.4% of the total weighed abundances) and *Sphingomonas* (19.4%), making up together for more than 40% of the total weighted abundance. The following two taxa, *Beijerinckia* (5.5%) and *Phenylobacterium* (4.5%), are already much rarer.

The 18S nuc rDNA barcode of the dark-spored myxomycetes was successfully amplified for six out of eight samples of the DNA isolated from resin. Among the 50 most abundant ASVs, 18 ASVs summing up to 67.3% of all reads had *Diacheopsis resinae* as best matches

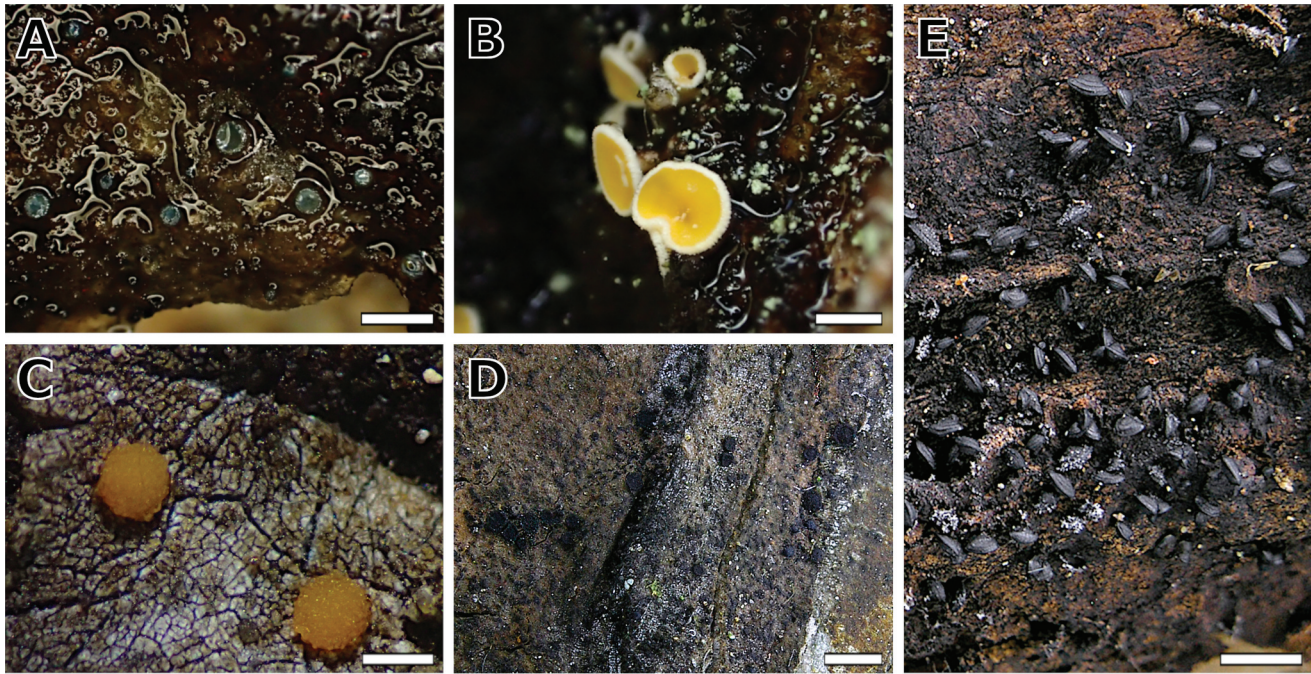


Figure 5. Resiniculous ascomycetes associated with *Diacheopsis resiniae* in the Black Forest National Park. (A) *Claussenomyces* sp. (KR-M-0093597). (B) *Lachnellula resinaria* (KR-M-0093592). (C) *Zythia resiniae* on resin of *Picea abies* (KR-M-0093519). (D) *Sarea difformis* (KR-M-0092716). (E) *Lophium mytilinum* (KR-M-0093592). Images A–C: F. Popa, D–E: M. Theiss. Bars: A, E = 2 mm; B–D = 1 mm.

Table 1. Most common species observed in all eight samples and/or metabarcoding with fungal (F) ITS2 and bacterial (B) 16S rDNA primers.

Species	Reference sequence	OTU	Reads × Frequency	Voucher
<i>Sarea difformis</i> (F)	GBSO8071-13 (100.0%, B)	3	371 744	3591
<i>Infundichalara microchona</i> (F)	GBHEL1084-13 (99.3%, B)	5	351 264	3632
<i>Lophium arboricola</i> (F)	GBSO8073-13 (98.7%, B)	4	339 000	3590, 3591
<i>Sorocybe resiniae</i> (F)	GBF020-08 (98.7%, B)	2	292 400	3590, 3591
<i>Zythia resiniae</i> (F)	GBSO13500-15 (98.9%, B)	1	183 976	3591
<i>Chaetothyriales</i> sp. (F)	GBSO3456-13 (84.4%, B)	7	149 288	—
<i>Herpotrichiellaceae</i> sp. (F)	UDB0486015 (100.0%, B)	11	147 672	—
uncultured fungus (F)	KU061857 (99.3%, G)	6	136 496	—
<i>Lachnellula resinaria</i> (F)	MT913605 (97.9%, G)	15	45 232	3592
<i>Lophium mytilinum</i> (F)	GBPLE908-13 (100.0%, B)	20	36 856	3591
<i>Claussenomyces</i> sp. (F)	KY689630 (99.6%, G), KY661433 (99.6%, G)*	38, 55	2700, 1041	3597
<i>Endobacter</i> sp. (B)	JF217150 (99.5%, S)	2	213 048	—
<i>Sphingomonas</i> sp. (B)	AM697454 (100.0%, S)	1	193 232	—

Note. Total number of reads × frequency among the eight samples >100 000 (for a list of all sequences, refer to SUPPLEMENTARY FILE 8). Given are taxon names and reference sequences from the databases BOLD (B), GenBank (G), and SILVA (S) with the respective percent identity, OTU number, weighted abundance, and voucher specimens (the full number is KR-M-009xxxx, given are the last four digits). Species with an entry in “Reads × Frequency” were found in metabarcoding; those with a voucher number were visually detected (lens and/or compound microscope).

*No unambiguous assignment of a single species possible.

(SUPPLEMENTARY FILE 9). Three of them were identical to ribotypes from the clades *res1*, *res2a*, and *res2b*, another nine ASVs were closely related to the ribotypes known from fruit bodies, and six ASVs formed two new subclades within *Diacheopsis resiniae* (SUPPLEMENTARY FIG. 6). Each sample yielded between 2 and 14 different ASVs assigned to *Diacheopsis resiniae*. The remaining 32 ASVs were assigned to genera *Badhamia*, *Comatricha*, *Diacheopsis*, and *Lamproderma* (SUPPLEMENTARY FILE 9).

DISCUSSION

Genera within Lamprodermataceae.—With 58 currently described species, the genus *Lamproderma*, described already by Rostafinski (1873), is one of the most diverse in myxomycetes, surpassed only by *Diderma* (ca. 85 accepted taxa; Lado et al. 2005–2023; Novozhilov, Prikhodko et al. 2022), *Didymium* (more than 90 recognized species taxa; Zamora et al. 2023), and *Physarum* (ca. 160 taxa; García-Martín et al. 2023; Prikhodko, Shchepin,

Gmoshinskiy et al. 2023). Most species of *Lamproderma* are nivicolous (Schnittler et al. 2015) or bryophilous, preferring cool and shaded microhabitats (Stephenson and Studlar 1985). Morphologically the genus is clearly characterized (Dennison 1945a, 1945b): stalked sporocarps with a blunt columella and a radiating capillitium that is not tightly connected to the thin, membranous, and often iridescent peridium, which persists for a rather long time after irregular dehiscence; lime absent or only in traces (flakes in *Lamproderma pulveratum*, or splinters in *L. arcyrioides*, *L. maculatum*, and *L. pseudomaculatum*). Unfortunately, all phylogenies let the genus appear as paraphyletic (FIG. 1 herein and Fiore-Donno et al. 2012, complete 18S nuc rDNA sequences). *Lamproderma cacographicum* appears as the most basal species, and Physaraceae and Didymiaceae are nested in the clade accompanying all other *Lamproderma* spp., together with *Elaeomyxa*, and the sessile genera *Colloderma* and *Diacheopsis*. A recent three-gene phylogeny with focus on Didymiaceae (Prikhodko, Shchepin, Bortnikova et al. 2023) confined this; we thus have a situation similar to that in Physaraceae (García-Martín et al. 2023; Prikhodko, Shchepin, Gmoshinskiy et al. 2023). This problem remains after former emendations of the genus: *L. arcyrioides*, now *Collaria arcyrioides* (Nannenga-Bremekamp 1967), was excluded from *Lamproderma* spp., and the *L. atrosporum* group was recognized as in its own genus —*Meriderma* (Poulain et al. 2011), which assumes the most basal position within dark-spored myxomycetes (Feng et al. 2016; Fiore-Donno et al. 2012).

The three remaining genera of the Lamprodermataceae sensu Leontyev et al. (2019), *Colloderma*, *Diacheopsis*, and *Elaeomyxa*, include mostly rare species: the material available in collections is usually scanty, often old, and sometimes allows sequencing only the 18S nuc rDNA marker. In the tree of this barcoding marker targeting the genera *Diacheopsis* and *Lamproderma* (SUPPLEMENTARY FIG. 4), deeper branches are often not well supported, but many terminal clades with high support are helpful for species delimitation. The main characters delimiting *Diacheopsis* from *Lamproderma* are the “absent” ones: the lacking stalk and columella. From the 19 described *Diacheopsis* spp., eight were barcoded, but we often could access only single specimens. Well-represented is only *D. metallica*, the most common species: its barcode cannot be distinguished from those of *L. arcyrioides*, *L. cristatum*, *L. pulveratum*, and *L. spinulosporum* (SUPPLEMENTARY FIG. 4; SUPPLEMENTARY TABLE 1). This species seems essentially to be a sessile *Lamproderma*, and further investigations including more genetic markers are needed to disentangle this species complex. Obviously, the absence of a structure (in this case, the stalk) is not a useful character

for delimiting higher taxa, as already postulated by Eliasson (1977) for the absence of a capillitium defining the classical Liceales (see discussion in Leontyev et al. 2019).

We need a critical revision of Lamprodermataceae to justify and delimit its genera, but the results of this study allow the following major conclusions:

- (I) New traits must be found to delimit genera, and due to often convergent evolution, such characters may be absent or at least not obvious. This requires comprehensive taxon sampling in further studies.
- (II) Barcoding often, but not always, works reliably (Borg Dahl et al. 2018; Schnittler et al. 2017, 2020). As stated in Yatsiuk et al. (2023), a barcoding gap that fits all dark-spored myxomycetes does not exist, and contradictions between barcoding and morphological differentiation must be examined using multiple genetic markers.
- (III) We must deal with numerous taxa that are hard to characterize, as they rarely fruit (or even never, as hypothesized in Shchepin et al. 2019), since the fruiting propensity of myxomycete species may be very different in general, not only between habitats or regions. *Diacheopsis* spp. seems to be a prominent example (except for *D. metallica*).

In spite of these yet unsolved problems, we decided to describe the new, clearly delimited taxon still under the generic name *Diacheopsis*, since (i) molecular data are not yet sufficient to decide on a new generic classification of Lamprodermataceae, and (ii) according to the morphological species concept, upon which most of the field observations and ecological studies are based, the new species can be unambiguously accommodated under this name.

Circumscription of *D. Resinae*.—The phylogeny (FIG. 1) of two independent genetic markers showed a clear split into two phylogroups (*res1* and *res2*), one of them splitting into two more subgroups (*res2a* and *res2b*). All three groups received maximum statistical support. The recombination analysis (FIG. 2) reveals that these three groups (one called *res1a* in FIG. 1 and *res1* in FIG. 2; *res2a* and *res2b*) are reproductively isolated, with a single exception of one *EF1α* allele shared by some specimens from *res1* and *res2a* that might be explained by incomplete lineage sorting, which is not unusual

among closely related species. In addition, we found no morphological or ecological characters discriminating between these three groups. We therefore decided to describe all three groups under the name *D. resinae*, although further investigations with more available material might change this pattern.

The existence of several biological species within one morphospecies is not uncommon for myxomycetes and was documented in several studies via tests for reproductive isolation with independently inherited marker genes (*Trichia varia*, Feng and Schnittler 2015; *Hemitrichia serpula*, Dagamac et al. 2017; *Physarum albescens*, Shchepin et al. 2022; *Didymium nivicola*, Janik et al. 2020; *Lycogala epidendrum*, Leontyev et al. 2022; *Diderma* spp., Shchepin et al. 2024). Another case where different ecological niches suggest biological speciation is *Badhamia melanospora* (Aguilar et al. 2014). This differentiation may or may not be accompanied by subtle morphological differences (not found for *T. varia*; details of spore ornamentation visible in SEM only for *H. serpula*; peridium and lime node coloration differing in *P. albescens*). For *Lycogala epidendrum* (Leontyev et al. 2022), a whole set of newly discovered microscopic characters allows morphological description of at least a part of the newly discovered species (Leontyev et al. 2023). The delimitation of nine new taxa in the polyphyletic *Trichia botrytis* complex is a similar case, since the taxonomic value of several morphological characters was reevaluated with support from molecular phylogenies (Bortnikov et al. 2023).

In most of these cases, the biospecies have not been formally described at any taxonomic rank, since they cannot be differentiated without considerable additional effort. A case where a molecular differentiation was successfully proven to be accompanied by differences in microscopic characters concerns *Didymium nivicola* and *D. pseudonivicola* (Janik et al. 2020, 2021).

For *Diacheopsis resinae*, the differences in spore size between the phylogroups (putative biospecies) are not significant (SUPPLEMENTARY FIG. 2). As stated in Woyzichovski et al. (2022) for *Ph. albescens*, variation due to environmental plasticity may overrule genetically coded differences, even if these exist between the phylogroups in *D. resinae*. Taking into account that the biospecies of *D. resinae* show no geographic segregation and share the same ecological niche, we describe only one species. We have chosen the holotype from the phylogroup *res2a* and cite other studied specimens of the same ribogroup to enable later emendations, if future research will show the phylogroups to represent separate species.

Ecology.—The new species (or complex of biological species) occupies an ecological niche not yet discovered for myxomycetes: stem wounds of coniferous trees with resin flow. The resin of coniferous trees contains a high diversity of secondary metabolites inhibiting the colonization by fungi and bacteria (Pearce 1996). Only a highly specific community of fungal species is able to colonize this substrate (Mitchell et al. 2021; Roll-Hansen and Roll-Hansen 1980). The fungi observed together with *D. resinae* are known to occur on conifer resin (Roll-Hansen and Roll-Hansen 1980; Seifert et al. 2007). *Infundichalara microchona* was also described growing on decayed coniferous wood and fruit bodies of Polyporales (Réblová and Štěpánek 2011). The apothecia of *Sarea difformis*, *Zythia resinae*, and *Lachnellula resinaria* together with the mononematous and synnematous blackish anamorphs of “*Sorocybe resinae*” (stalked, black conidiophores) can be used as indicators for the potential presence of *Diacheopsis resinae*, although we do not assume a direct link, such as a trophic relationship, between the myxomycetes and the fungi.

The continuity and high abundance of sequence reads of the two bacterial genera *Endobacter* and *Sphingomonas* indicates a possible link between *Diacheopsis resinae* and species of the two bacterial genera, which may constitute the main food source for amoebae and/or plasmodia.

In contrast, the phenology of the new species seems to be determined by precipitation and temperature. It shows a clear fructification peak in the winter months (February; SUPPLEMENTARY FIG. 3) when the evapotranspiration is lowest and the bark stays wet over longer periods of time. We thus can conclude that it can develop at low temperatures (a feature the new taxon shares with related nivicolous species of *Lamproderma* and *Diacheopsis*). However, it seems also to be able to tolerate frosts. This contrasts with myxamoebae of nivicolous species, which develop at low but positive temperatures beneath the snow (Borg Dahl et al. 2019; Schnittler et al. 2015) and will die with sudden cold spells (Shchepin et al. 2014). The vertical habitat of *D. resinae* is not insulated by a thick snow cover and will be exposed to frost, even sudden frosts—many records were found above 1 m height.

In contrast to corticolous species (Mitchell 1978a, 1978b, 1979), which develop on the outer, dead bark of living trees, our species seems to be confined to stem wounds. Therefore, it was never detected in the thousands of moist chamber cultures set up with bark of living trees (e.g., Härkönen and Ukkola 2000).

Summarizing, this study illustrates the challenges that protist taxonomy faces in the molecular age:

morphological concepts of genera and species are shattered by molecular results, since we have only a limited display of morphological characters to compare, and especially conspicuous characters may be the result of convergent evolution, as it is most likely the case for compound fructifications (see discussion in Leontyev et al. 2019). In addition, myxomycetes are sexual amoebae (see discussion in Lahr et al. 2011; Spiegel 2011), like all Eukaryotes (Hofstatter and Lahr 2019), and seem to possess a mechanism by which morphologically circumscribed species segregate into reproductively isolated units we can call biological species (see discussion in Feng et al. 2016; Feng and Schnittler 2015). As such, future field surveys and morphological studies in this group need to be accompanied by molecular investigations. With this combination of methods, in spite of more than 200 years of field research in myxomycetes (Stephenson et al. 2008), there is still a lot to discover, as this study shows.

ACKNOWLEDGMENTS

We acknowledge support of the authorities from the Black Forest National Park, D-77889 Seebach, Germany. Dr. M. Theiss provided the images of *Lophium mytilinum*. For help with SEM images, we wish to thank Prof. G. Moreno (University of Alcalá, Spain), A. Priego and J. A. Pérez (Electron Microscopy Service of the University of Alcalá). Dr. Jean Cavaillon, president of the “Société Mycologique Centre Alsace,” provided a specimen from Saint Hippolyte (BW3538). Edvin W. Johannesen and Per Vetlesen, Norway, helped with information on the Norwegian finds. H.F.G. is grateful to Niels V. Mogensen, who suggested the excursion that in the first place led to the discovery of the new species, and who accompanied H.F.G. on numerous other excursions in pursuit of more finds. We acknowledge the use of equipment of the Core Facility Center “Cell and Molecular Technologies in Plant Science” at the Komarov Botanical Institute RAS (St. Petersburg). Finally, all authors thank several reviewers for their helpful comments.



DISCLOSURE STATEMENT

No potential conflict of interest was reported by the author(s).

FUNDING

Additional sequences of Physarales were generated by Y.K.N. and I.S.P. within the project of the Komarov Botanical Institute RAS, grants [12401310-0829-3 and 075-15-2021-1056]. Molecular work on the new species was funded in part by the German Research Foundation under the grants [RTG 2010 and SCHN1080/6-1] to M.S.

ORCID

Flavius Popa  <http://orcid.org/0000-0002-1857-7372>
 Oleg N. Shchepin  <http://orcid.org/0000-0001-9327-7655>
 Ilya S. Prikhodko  <http://orcid.org/0000-0001-7383-0302>
 Ángela López-Villalba  <http://orcid.org/0000-0003-0166-8224>
 Yuri K. Novozhilov  <http://orcid.org/0000-0001-8875-2263>
 Martin Schnittler  <http://orcid.org/0000-0003-0909-5627>

LITERATURE CITED

- Aguilar M, Fiore-Donno A-M, Lado C, Cavalier-Smith T. 2014. Using environmental niche models to test the ‘everything is everywhere’ hypothesis for *Badhamia*. ISME J. 8 (4):737–745. doi:10.1038/ismej.2013.183.
- Asbeck T, Benneter A, Huber A, Margaritis D, Buse J, Popa F, Pyttel P, Förschler M, Gärtner S, Bauhus J. 2023. Enhancing structural complexity: an experiment conducted in the Black Forest National Park, Germany. Ecol Evol. 13: e9732. doi:10.1002/ece3.9732.
- Boehm E, Mugambi GK, Miller A, Huhndorf SM, Marincowitz S, Spatafora J, Schoch C. 2009. A molecular phylogenetic reappraisal of the Hysteriaceae, Mytiliniaceae and Gloniaceae (Pleosporomycetidae, Dothideomycetes) with keys to world species. Stud Mycol. 64:49–83. doi:10.3114/sim.2009.64.03.
- Borg Dahl M, Brejnrod AD, Russel J, Sørensen SJ, Schnittler M. 2019. Different degrees of niche differentiation for bacteria, fungi and myxomycetes within an elevational transect in the German Alps. Microbial Ecol. 78 (3):764–780. doi:10.1007/s00248-019-01347-1.
- Borg Dahl M, Brejnrod AD, Unterseher M, Hoppe T, Feng Y, Novozhilov YK, Sørensen SJ, Schnittler M. 2018. Genetic barcoding of dark-spored myxomycetes (Amoebozoa) – identification, evaluation and application of a sequence similarity threshold for species differentiation in NGS studies. Mol Ecol Res. 18:306–318. doi:10.1111/1755-0998.12725.
- Bortnikov FM, Bortnikova NA, Gmshinskiy VI, Prikhodko IS, Novozhilov YK. 2023. Additions to *Trichia botrytis* complex (Myxomycetes): 9 new species. Botanica Pacifica. [accessed 2023 Jul 26]:[39 p.]. doi:10.17581/bp.2023.12s03.
- Dagamac NHA, Rojas C, Novozhilov YK, Moreno GH, Schlueter R, Schnittler M. 2017. Speciation in progress? A phylogeographic study among populations of *Hemitrichia serpulula* (Myxomycetes). PLOS ONE. 12: e0174825. doi:10.1371/journal.pone.0174825.
- Dennison ML. 1945a. The genus *Lamproderma* and its relationships. I. Mycologia. 37:80–108. doi:10.1080/00275514.1945.12023971.
- Dennison ML. 1945b. The genus *Lamproderma* and its relationships. II. Mycologia. 37:197–203. doi:10.1080/00275514.1945.12023981.
- Doyle JJ. 1995. The irrelevance of allele tree topologies for species delimitation, and a non-topological alternative. Syst Bot. 20:574–588. doi:10.2307/2419811.
- Eliasson UH. 1977. Recent advances in the taxonomy of Myxomycetes. Botaniska Notiser. 130:483–492.
- Ellis MB, Ellis JP. 1985. Microfungi on land plants. An identification handbook. London: Croom Helm. p. 818.

- Feng Y, Klahr A, Janik P, Ronikier A, Hoppe T, Novozhilov YK, Schnittler M. 2016. What an intron may tell: several sexual biospecies coexist in *Meriderma* spp (Myxomycetes). *Protist*. 167:234–253. doi:10.1016/j.protis.2016.03.003.
- Feng Y, Schnittler M. 2015. Sex or no sex? Group I introns and independent marker genes reveal the existence of three sexual but reproductively isolated biospecies in *Trichia varia*. (Myxomycetes). *Organisms Divers Evol*. 15:631–650. doi:10.1007/s13127-015-0230-x.
- Fiore-Donno AM, Kamono A, Meyer M, Schnittler M, Fukui M, Cavalier-Smith T. 2012. 18S rDNA phylogeny of *Lamproderma* and allied genera (Stemonitales, Myxomycetes, Amoebozoa). *PLOS ONE*. 7(e35359). doi:10.1371/journal.pone.0035359.
- Fiore-Donno AM, Meyer M, Baldauf SL, Pawlowski J. 2008. Evolution of dark-spored Myxomycetes (slime-molds): molecules versus morphology. *Mol Phylogenet Evol*. 46:878–889. doi:10.1016/j.ympev.2007.12.011.
- Fiore-Donno AM, Novozhilov YK, Meyer M, Schnittler M. 2011. Genetic structure of two protist species (Myxogastria, Amoebozoa) reveals possible predominant asexual reproduction in sexual amoebae. *PLOS ONE*. 6:e22872. doi:10.1371/journal.pone.0022872.
- Fiore-Donno AM, Tice AK, Brown MW. 2018. A non-flagellated member of the Myxogastria and expansion of the Echinosteliida. *J Eukaryot Microbiol*. 66:538–544. doi:10.1111/jeu.12694.
- Flot J-F, Couloux A, Tillier S. 2010. Haplowebs as a graphical tool for delimiting species: a revival of Doyle's "field for recombination" approach and its application to the coral genus *Pocillopora* in Clipperton. *BMC Evol Biol*. 10:372. doi:10.1186/1471-2148-10-372.
- García-Martín JM, Zamora JC, Lado C. 2023. Multigene phylogeny of the order Physarales (Myxomycetes Amoebozoa): shedding light on the dark-spored clade. *Persoonia*. 51:89–124. doi:10.3767/persoonia.2023.51.02.
- Hansen L, Knudsen K. 2000. *Nordic Macromycetes*. Vol. 1. Ascomycetes. Copenhagen (Denmark): Nordsvamp. p. 309.
- Härkönen M, Ukkola T. 2000. Conclusions on Myxomycetes compiled over Twenty-Five years from 4793 moist chamber cultures. *Stapfia*. 73. <https://archive.org/details/stapfia-73-105-112>.
- Hausmann A, Segerer AH, Greifenstein T, Knubben J, Morinière J, Bozicevic V, Doczkal D, Günter A, Ulrich W, Habel JC. 2020. Toward a standardized quantitative and qualitative insect monitoring scheme. *Ecol Evol*. 10(9):4009–4020. doi:10.1002/ece3.6166
- Hawksworth D, Sherwood MA. 1981. A reassessment of three widespread resinicolous discomycetes. *Canadian J Bot*. 59(3):357–372. doi:10.1139/b81-049.
- Hoang DT, Chernomor O, von Haeseler A, Minh BQ, Vinh LS. 2018. UFBoot2: improving the Ultrafast Bootstrap Approximation. *Mol Biol Evol*. 35(2):518–522. doi:10.1093/molbev/msx281.
- Hofstätter PG, Lahr DJG. 2019. All Eukaryotes are sexual, unless proven otherwise: many so-called asexuals present meiotic machinery and might be able to have sex. *Bioessays*. 41(6):e1800246. doi:10.1002/bies.201800246.
- Huelsenbeck JP, Ronquist F. 2001. MrBayes: Bayesian inference of phylogeny. *Bioinformatics*. 17:754–755. doi:10.1093/bioinformatics/17.8.754.
- Janik P, Lado C, Ronikier A. 2020. Range-wide phylogeography of a nivicolous protist *Didymium nivicola* Meyl. (Myxomycetes, Amoebozoa): striking contrasts between the Northern and the Southern Hemisphere. *Protist*. 171(6):125771. doi:10.1016/j.protis.2020.125771.
- Janik P, Szczepaniak M, Lado C, Ronikier A. 2021. *Didymium pseudonivicola*: a new myxomycete from the austral Andes emerges from broad-scale morphological and molecular analyses of *D. nivicola* collections. *Mycologia*. 113(6):1327–1342. doi:10.1080/00275514.2021.1961068.
- Kalyaanamoorthy S, Minh BQ, Wong TKF, von Haeseler A, Jermiin LS. 2017. ModelFinder: fast model selection for accurate phylogenetic estimates. *Nat Methods*. 14:587–589. doi:10.1038/nmeth.4285.
- Katoh K, Rozewicki J, Yamada KD. 2019. MAFFT online service: multiple sequence alignment, interactive sequence choice and visualization. *Brief Bioinform*. 20(4):1160–1166. doi:10.1093/bib/bbx108.
- Katoh K, Standley DM. 2013. MAFFT Multiple Sequence Alignment Software Version 7: improvements in Performance and Usability. *Mol Biol Evol*. 30:772–780. doi:10.1093/molbev/mst010.
- Kowalski DT. 1968. Observations on the genus *Lamproderma*. *Mycologia*. 60:756–768. doi:10.1080/00275514.1968.12018636.
- Kowalski DT. 1970. The species of *Lamproderma*. *Mycologia*. 62:621–672. doi:10.1080/00275514.1970.12019010.
- Kowalski DT. 1975. The myxomycete taxa described by Charles Meylan. *Mycologia*. 67:448–494. doi:10.1080/00275514.1975.12019774.
- Lado C. 2005–2023. An on-line nomenclatural information system of Eumycetozoa. [accessed 2023 Jul 20]. <http://www.eumycetozoa.com>
- Lahr DJG, Parfrey LW, Mitchell EA, Katz LA, Lara E. 2011. The chastity of amoebae: re-evaluating evidence for sex in amoeboid organisms. *Proc R Soc B*. 278:2081–2090. doi:10.1098/rspb.2011.0289.
- Leontyev DV, Buttgerit M, Kochergina A, Shchepin ON, Schnittler M. 2023. Two independent genetic markers support separation of the myxomycete *Lycogala epidendrum* into numerous biological species. *Mycologia*. 115(1):32–43. doi:10.1080/00275514.2022.2133526.
- Leontyev DV, Schnittler M, Ishchenko Y, Quade A, Kahlert H, Rojas Alvarado C, Stephenson SL, Kochergina AV. 2022. Another species complex in myxomycetes: diversity of peridial structures in *Lycogala epidendrum*. *Nova Hedwigia*. 114(3–4):413–434. doi:10.1127/nova_hedwigia/2022/0690.
- Leontyev DV, Schnittler M, Stephenson SL, Novozhilov YK, Shchepin ON. 2019. Towards a phylogenetic classification of the Myxomycetes. *Phytotaxa*. 399:209–238. doi:10.11646/phytotaxa.399.3.5.
- López-Villalba A, Moreno G, Tapia M. 2022. Nivicolous myxomycetes from the Navarran and French Pyrenees. *Mycotaxon*. 137:359–369. doi:10.5248/137.359.
- Martin GW, Alexopoulos CJ. 1969. *The Myxomycetes*. Iowa City: University of Iowa Press. p. 560 + 41pl.

- Martin M. 2011. Cutadapt removes adapter sequences from high-throughput sequencing reads. *EMBnet. Journal*. 17(1):10–12. doi:10.14806/ej.17.1.200.
- Météo-France. 2023. [accessed 2023 Jan 1]. <https://www.infoclimat.fr/climatologie/normales-records/1981-2010/moutherhouse/valeurs/57489001.html>
- Meylan C. 1908. Contributions à la connaissance des Myxomycètes du Jura. *Bull Soci Vaudoise Sci Nat*. 44:285. <https://www.e-periodica.ch/digbib/view?pid=bsv-002%3A1908%3A44%3A%3A321#321>.
- Meylan C. 1930. Note sur un nouveau genre de Myxomycètes. *Bull Soc Vaudoise Sci Nat*. 57:147–149. <https://www.e-periodica.ch/digbib/view?pid=bsv-002%3A1929%3A57%3A%3A157#157>.
- Miller MA, Pfeiffer W, Schwartz T. 2010. Creating the CIPRES Science Gateway for inference of large phylogenetic trees. *Gateway Comput Environ Workshop (GCE)*:1–8. <https://doi.org/10.1109/GCE.2010.5676129>
- Mitchell DW. 1978a. A key to the corticolous myxomycetes. Part I. *Bull Br Mycol Soc*. 12(1):18–42. doi:10.1016/S0007-1528(78)80007-8.
- Mitchell DW. 1978b. A key to the corticolous myxomycetes. Part II. *Bull Br Mycol Soc*. 12(2):90–107. doi:10.1016/S0007-1528(78)80029-7.
- Mitchell DW. 1979. A key to the corticolous myxomycetes. Part III. *Bull Br Mycol Soc*. 13(1):42–60. doi:10.1016/S0007-1528(79)80046-2.
- Mitchell JK, Garrido-Benavent I, Quijada L, Pfister DH. 2021. *Sareomycetes*: more diverse than meets the eye. *IMA Fungus*. 12:6. doi:10.1186/s43008-021-00056-0.
- Morinière J, Cancian de Araujo B, Lam AW, Hausmann A, Balke M, Schmidt S, Hendrich L, Doczkal D, Fartmann B, Arvidsson S, et al. 2016. Species identification in malaise trap samples by DNA barcoding based on NGS technologies and a scoring matrix. *PLOS ONE*. 11(5):e0155497. doi:10.1371/journal.pone.0155497.
- Nannenga-Bremekamp NE 1967. Notes on Myxomycetes. XII. A revision of the Stemonitales. *Proceedings of the Koninklijke Nederlandse Akademie van Wetenschappen. Series C*. 70:201–216.
- Nguyen LT, Schmidt HA, von Haeseler A, Minh BQ. 2015. IQ-TREE: a fast and effective stochastic algorithm for estimating maximum-likelihood phylogenies. *Mol Biol Evol*. 32(1):268–274. doi:10.1093/molbev/msu300.
- Novozhilov YK, Okun MV, Erastova DA, Shchepin ON, Zemlyanskaya IV, García-Carvajal E, Schnittler M. 2013. Description, culture and phylogenetic position of a new xerotolerant species of *Physarum*. *Mycologia*. 105:1535–1546. doi:10.3852/12-284.
- Novozhilov YK, Prikhodko IS, Fedorova NA, Shchepin ON, Gmshinskiy VI, Schnittler M. 2022. *Lamproderma vietnamense*: a new species of myxomycetes with reticulate spores from Phia Oắc – phia Đén National Park (northern Vietnam) supported by molecular phylogeny and morphological analysis. *Mycoscience*. 63:149–155. doi:10.47371/mycosci.2022.05.003.
- Novozhilov YK, Shchepin ON, Prikhodko IS, Schnittler M. 2022. A new nivicolous species of *Diderma* (Myxomycetes) from Kamchatka, Russia. *Nova Hedwigia*. 114(1–2):181–196. doi:10.1127/nova_hedwigia/2022/0670.
- Okonechnikov K, Golosova O, Fursov M, UGENE Team. 2012. Unipro UGENE: a unified bioinformatics toolkit. *Bioinformatics*. 28:1166–1167. doi:10.1093/bioinformatics/bts091.
- Pearce R. 1996. Antimicrobial defenses in the wood of living trees. *New Phytologist*. 132:203–233. doi:10.1111/j.1469-8137.1996.tb01842.x.
- Poulain M, Meyer M, Bozonnet J. 2011. *Les Myxomycètes*. Vol. 1 & 2. Sevrier (France): Fédération mycologique et botanique Dauphine-Savoie. p. 568 + 544 pl.
- Prikhodko IS, Shchepin ON, Bortnikova NA, Novozhilov YK, Gmshinskiy VI, Moreno G, López-Villalba Á, Stephenson SL, Schnittler M. 2023. A three-gene phylogeny supports taxonomic rearrangements in the family Didymiaceae (Myxomycetes). *Mycol Prog*. 22(2):11. doi:10.1007/s11557-022-01858-1.
- Prikhodko IS, Shchepin ON, Gmshinskiy VI, Schnittler M, Novozhilov YK. 2023. Reassessing the phylogenetic position of the genus *Kelleromyxa* (Myxomycetes) using genome skimming data. *Protistology*. 17(2):73–84. doi:10.21685/1680-0826-2023-17-2-2.
- Rambaut A, Drummond AJ, Xie D, Baele G, Suchard MA. 2018. Posterior summarisation in Bayesian phylogenetics using Tracer 1.7. *Syst Biol*. 67:901–904. doi:10.1093/sysbio/syy032.
- Réblová M, Štěpánek V. 2011. The new hyphomycete genera *Brachyalara* and *Infundichalara*, the similar *Exochalara* and species of '*Phialophora* sect *Catenulatae*' (Leotiomyces). *Fungal Diversity*. 46:67–86. doi:10.1007/s13225-010-0077-6.
- Rognes T, Flouri T, Nichols B, Quince C, Mahé F. 2016. VSEARCH: a versatile open source tool for metagenomics. *PeerJ*. 4:e2584. doi:10.7717/peerj.2584.
- Roll-Hansen F, Roll-Hansen H. 1980. Microorganisms which invade *Picea abies* in seasonal stem wounds. *Forest Pathol*. 10(7):396–410. doi:10.1111/j.1439-0329.1980.tb00057.x.
- Ronikier A, García-Cunchillos I, Janik P, Lado C. 2020. Nivicolous Trichiales from the austral Andes: unexpected diversity including two new species. *Mycologia*. 112:753–780. doi:10.1080/00275514.2020.1759978.
- Ronikier A, Janik P, de Haan M, Kuhnt A, Zankowicz M. 2022. Importance of type specimen study for understanding genus boundaries—taxonomic clarifications in *Lepidoderma* based on integrative taxonomy approach leading to resurrection of the old genus *Polyschismium*. *Mycologia*. 114:1008–1031. doi:10.1080/00275514.2022.2109914.
- Ronikier A, Ronikier M. 2009. How 'alpine' are nivicolous myxomycetes? A worldwide assessment of altitudinal distribution. *Mycologia*. 101:1–16. doi:10.3852/08-090.
- Rostafiński J. 1873. Versuch eines Systems der Mycetozoen. Inaugural dissertation. Strassburg: University Press. p. 115.
- Schnittler M, Dagamac NHA, Leontyev DL, Shchepin ON, Novozhilov YK, Klahr A. 2020. Quick n' Cheap – a simplified workflow to barcode plasmodial slime molds (Myxomycetes). *Karstenia*. 58(2):393–400. doi:10.29203/ka.2020.505.
- Schnittler M, Erastova DA, Shchepin ON, Heinrich E, Novozhilov YK. 2015. Four years in the Caucasus – observations on the ecology of nivicolous myxomycetes. *Fungal Ecol*. 14:105–115. doi:10.1016/j.funeco.2015.01.003.

- Schnittler M, Shchepin ON, Dagamac NHA, Borg Dahl M, Novozhilov YK. 2017. Barcoding myxomycetes with molecular markers: challenges and opportunities. *Nova Hedwigia*. 104:323–341. doi:10.1127/nova_hedwigia/2017/0397.
- Seifert KA, Hughes SJ, Boulay H, Louis-Seize G. 2007. Taxonomy, nomenclature and phylogeny of three cladospore-like hyphomycetes, *Sorocybe resinae*, *Seifertia azalea* and the *Hormoconis* anamorph of *Amorphotheca resinae*. *Stud Mycol*. 58:235–245. doi:10.3114/sim.2007.58.09.
- Shchepin ON. 2021. Visualization of recombination patterns [Source code]. GitHub. [accessed 2023 July 24] https://github.com/Gurdhhu/recombination_graph/
- Shchepin ON. 2023. Python script for deriving haplotypes from aligned unphased sequences [Source code]. GitHub. [accessed 2023 July 24] https://github.com/Gurdhhu/get_haplotypes/
- Shchepin ON, López Villalba Á, Inoue M, Prikhodko IS, Erastova DA, Okun MV, Woyzichovski J, Yajima Y, Gmshinskiy VI, Moreno G, et al. 2024. DNA barcodes reliably differentiate between nivicolous species of *Diderma* (Myxomycetes, Amoebozoa) and reveal regional differences within Eurasia. *Protist*. 175:126023. doi:10.1016/j.protis.2024.126023.
- Shchepin ON, Novozhilov YK, Schnittler M. 2014. Nivicolous myxomycetes in agar culture: some results and open problems. *Protistology*. 8(2):53–61.
- Shchepin ON, Novozhilov YK, Woyzichovski J, Bog M, Prikhodko I, Fedorova N, Gmshinskiy V, Dahl MB, Dagamac NHA, Yajima Y, et al. 2022. Genetic structure of the protist *Physarum albescens* (Amoebozoa) revealed by multiple markers and genotyping by sequencing. *Mol Ecol*. 31(1):372–390. doi:10.1111/mec.16239.
- Shchepin ON, Schnittler M, Erastova DA, Prikhodko IS, Borg Dahl M, Azarov DV, Chernyaeva EN, Novozhilov YK. 2019. Community of dark-spored myxomycetes in ground litter and soil of taiga forest (Nizhne-Svirskiy Reserve, Russia) revealed by DNA metabarcoding. *Fungal Ecol*. 39:80–93. doi:10.1016/j.funeco.2018.11.006.
- Spiegel FW. 2011. Commentary on the chastity of amoebae: re-evaluating evidence for sex in amoeboid organisms. *Proc Soc. B*. 278:2096–2097. doi:10.1098/rspb.2011.0608
- Stephenson SL, Schnittler M, Novozhilov YK. 2008. Myxomycete diversity and distribution from the fossil record to the present. *Biodivers Conserv*. 17:285–301. doi:10.1007/978-90-481-2801-3_5.
- Stephenson SL, Studlar SM. 1985. Myxomycetes fruiting upon bryophytes: coincidence or preference? *Journal of Bryol*. 13:537–548. doi:10.1179/jbr.1985.13.4.537.
- Thijs S, Op De Beeck M, Beckers B, Truyens S, Stevens V, Van Hamme J, Weyens N, Vangronsveld J. 2017. Comparative evaluation of four Bacteria-specific primer pairs for 16S rRNA gene surveys. *Frontiers Microbiol*. 8:494. doi:10.3389/fmicb.2017.00494.
- Toju H, Tanabe AS, Yamamoto S, Sato H. 2012. High-Coverage ITS Primers for the DNA-Based Identification of Ascomycetes and Basidiomycetes in Environmental Samples. *PLOS ONE*. 7(7):e40863. doi:10.1371/journal.pone.0040863.
- Vaidya G, Lohman DJ, Meier R. 2011. SequenceMatrix: concatenation software for the fast assembly of multi-gene datasets with character set and codon information. *Cladistics*. 27:171–180. doi:10.1111/j.1096-0031.2010.00329.x.
- Vlasenko AV, Vlasenko VA, Kabilov MR. 2022. A new species of *Diacheopsis* from Russia. *Phytotaxa*. 541(2):193–200. doi:10.11646/phytotaxa.541.2.9.
- Woyzichovski J, Shchepin ON, Dagamac NHA, Schnittler M. 2021. A workflow for low-cost automated image analysis of myxomycete spore numbers, size and shape. *PeerJ*. 9:e12471. doi:10.7717/peerj.12471.
- Woyzichovski J, Shchepin ON, Schnittler M. 2022. High environmentally induced plasticity in spore size and numbers of nuclei per spore in *Physarum albescens* (Myxomycetes). *Protist*. 173(5):e12594. doi:10.1016/j.protis.2022.125904.
- Wrigley de Basanta D, Estrada-Torres A, García-Cunchillos I, Cano Echevarría A, Lado C. 2017. *Didymium azurellae*, a new myxomycete from cushion plants of cold arid areas of South America. *Mycologia*. 109:993–1002. doi:10.1080/00275514.2018.1426925.
- Yatsiuk I, Leontyev DL, López-Villalba Á, Schnittler M, Kõljalg U. 2023. A new nivicolous species of *Lamproderma* (Myxomycetes) from lowland and mountainous regions of Europe. *Nova Hedwigia*. 116(1–2):105–136. doi:10.1127/nova_hedwigia/2023/0807.
- Zamora JC, García-Martín JM, Lado C. 2023. (2955) Proposal to conserve the name *Didymium* against *Mucilago* and *Spumaria* (Physarales, Myxomycetes). *Taxon*. 72(3):663–664. doi:10.1002/tax.12964.